

Constellation-X Spectroscopy X-Ray Telescope Optical Assembly Pathfinder Image Error Budget and Performance Prediction

Dr. William A. Podgorski (SAO)

Co-authors:

Dr. Jay Bookbinder (SAO)
Dr. David Content (NASA/GSFC)
Mr. William Davis (SAO)
Mr. Mark Freeman (SAO)
Mr. Jason Hair (NASA/GSFC)
Dr. Scott Owens (NASA/GSFC)
Dr. Robert Petre (NASA/GSFC)
Dr. Paul Reid (SAO)
Dr. Timo Saha (NASA/GSFC)
Mr. Jeffrey Stewart (NASA/GSFC)
Dr. William Zhang (NASA/GSFC)

ABSTRACT

The Constellation-X mission is a follow-on to the current Chandra and XMM missions. It will place in orbit an array of four X-ray telescopes that will work in unison, having a substantial increase in effective area, energy resolution, and energy bandpass over current missions. To accomplish these ambitious increases new optics technologies must be exploited.

The primary instrument for the mission is the Spectroscopy X-Ray Telescope (SXT), which covers the 0.21 to 10 keV band with a combination of two x-ray detectors: a reflection grating spectrometer with CCD readout and a microcalorimeter. Mission requirements are an effective area of 15,000 cm² near 1 keV and a 15 arc-sec (HPD) image resolution with a goal of 5 arc-sec.

The Constellation-X SXT uses a segmented design with lightweight replicated optics. A technology development program is being pursued with the intent of demonstrating technical readiness prior to the program new start. Key elements of the program include the replication of the optical elements, assembly and alignment of the optics into a complete mirror assembly and demonstration of production techniques needed for fabrication of multiple units. These elements will be demonstrated in a series of engineering development and prototype optical assemblies which are increasingly flight-like.

In this paper we present image angular resolution error budgets for the SXT and for the Optical Assembly Pathfinder #2 (OAP2), the first of engineering development units intended to be tested in x-rays. We describe OAP2 image error sources and performance analyses made to assess error sensitivities. Finally we present an overall prediction of as-tested imaging performance in the x-ray test facility.

Keywords: X-Ray Optics, Optical Alignment, Constellation-X, Spectroscopy X-Ray Telescope, Centroid Detector Assembly

1. INTRODUCTION

The Constellation-X Spectroscopy X-Ray Telescope (SXT) is one of the key components under development for the Constellation-X mission. The SXT Flight Mirror Assembly (FMA) assembly is a multi-shell, segmented X-ray mirror assembly which also provides an interface and mounting structure for the reflection grating assembly (RGA) portion of the reflection grating spectrometer, thermal pre and post-collimators and thermal control components. To demonstrate our readiness to build the SXT, we have put in place a phased development program in which all the elements of the SXT will be developed and tested. This program features a series of increasingly flight-like engineering development and prototype test units¹. Broadly speaking, there are three major tasks involved in SXT development; optics and optic manufacturing, assembly and alignment and flight structure development. In the past year we have developed two Optical Assembly Pathfinders; OAP1 and OAP2. OAP1 is a mechanical pathfinder which was developed to test optical alignment procedures. OAP2 is a single-shell test unit intended for x-ray testing in the MSFC Stray Light Facility (SLF). In this paper we present both the flight SXT and the OAP2 image resolution error budgets. We describe OAP2 image error sources and performance analyses made to assess error sensitivities. Finally we present an overall prediction of as-tested imaging performance in the x-ray test facility. In §2 we present the flight SXT image resolution error budget. In §3 we discuss OAP2 requirements, design, assembly and alignment and in §4 we present the OAP2 image resolution error budget. In §5 we present OAP2-specific analytical results and an X-ray test image resolution performance prediction.

2. SXT FLIGHT MIRROR ASSEMBLY IMAGE ANGULAR RESOLUTION ERROR BUDGET

2.1 Overview of Flight SXT Top Level Error Budget

A top level performance requirement of the Constellation-X program is to have an image half power diameter (HPD) of 15 arc-seconds. The SXT Flight Mirror Assembly (FMA) image angular resolution error budget which supports this requirement is shown in Figure 1. Budget items are shown on the left in the “Contributors” column. Budget allocations and RSS sums (in red) are shown in the “Allocation” columns. Comments on the rationale for each item are in the right-hand column.

The budget is built from bottom to top, with lower level terms root-square-summing upwards and to the left. The starting point for this budget are the optical segments (9.9 arc-seconds HPD). A sub-budget for these elements is shown in Section 2.2, Table 1. Moving upwards on the error budget, an allocation is made for installation of the segments into the optical housing, prior to alignment. Our assembly process will be to install the elements into the optical housing and then, using ten active adjusters (5 top and 5 bottom), align the optic so that the images from all optic azimuths are coincident with each other and with the images from other shells. The installation process of the optics into the housing and adjusters creates errors which are captured in the “installation in housing” term. The next three terms (reading upwards) are errors associated with the assembly and alignment process. Alignment of the optics is done using the AXAF alignment sensor, the “Centroid Detector Assembly” (CDA). Static and dynamic alignment sensor errors, adjustment accuracy and errors due to thermal drift of the images during alignment are captured in the 3.38 arc-sec “alignment” allocation. These errors are discussed in Section XXXXX. After alignment, each segment is bonded into the optical housing. During this bonding process strains are introduced into the optics, primarily by epoxy shrinkage during cure. An allocation of 3 (HPD) arc-seconds is made for this “bonding strain error”. Working up in the budget, the next term is a “gravity release” term which is due to assembly in 1G (vertical optical axis) field and operation at zero G. An allocation of 1.5 arc-seconds is made for this term.

The term “SXT FMA, as built” is a roll-up term obtained by taking the RSS of the five terms below it. This term reflects the SXT performance after assembly and alignment but before installation into the telescope and launch.

Contributors (HPD - arcsec)	Rqmt	Margin	Allocations				Rationale	
RGS Resolution	15.00	3.92	14.48					4 satellites, post-processed
▪ Co-add 4 satellites				1.00				Superposition of data using X-ray centroids
▪ On-Orbit Telescope - single satellite				14.12				RSS
▪ CCD pixelization error				0.41				0.5 arcsec pixels
▪ Grating resolution error				3.00				Estimate
XMS Resolution	15.00	4.95	14.16					4 satellites, post-processed
Co-add 4 satellites				1.00				Superposition of data using X-ray centroids
On-Orbit Telescope - single satellite				14.12				RSS
▪ Calorimeter pixelization error					4.08			5 arcsec pixels
▪ Telescope level effects					5.20			RSS
- Image reconstruction errors (over obs)						4.24		RSS
- SXT/Telescope mounting strain						2.00		Eng. estimate based on Chandra experience
- SXT/SI vibration effects						2.00		Chandra experience (jitter)
- SXT/SI misalignment (off-axis error)						1.00		Chandra experience
- SXT/SI focus error						0.20		Analysis
▪ SXT FMA - on-orbit performance					12.48			RSS
- SXT FMA launch shifts						2.00		Eng. est. based on Chandra
- Thermal errors						2.24		RSS
- Material stability effects						1.00		Est. based on Chandra work
- SXT FMA, as built						12.07		RSS
-- Gravity release							1.50	FEA analysis using vertical assy
-- Bonding strain							3.00	Eng. estimate, analysis in process
-- Alignment errors (using CDA)							3.38	RSS
-- Installation in housing							5.00	Est. based on OAP1 testing
-- Optical elements							9.90	Est. based on tech dev program

Figure 1 - SXT Image Resolution Error Budget

The three terms above the “SXT FMA, as built” term are errors associated with launch and operation of the SXT in the on-orbit environment. An allocation of one arc-second is made for “Material stability effects”. These include both short and long term instabilities in the SXT materials. An example of such an effect would be strains developed in the replication epoxy due to out-gassing in the vacuum environment. Another example would be long-term creep of metallic materials used in the SXT housing. The “Thermal errors” term, 2.24 arc-seconds HPD, captures errors associated with operation of the SXT in a non-ideal thermal environment. The SXT will be manufactured in a temperature-controlled facility with one degree C control. When operating in space the SXT thermal control system will attempt to control the SXT overall temperature to the assembly temperature. Typical control tolerances are within one degree C of the set-point. This temperature difference will cause strains in the materials of the SXT with consequent performance impacts. The temperature control system will also attempt to maintain a uniform temperature throughout the SXT. In practice, this control is not perfect, and spatial thermal gradients will be present at some level within the SXT. These gradients also cause performance errors. The effects of both average temperature errors (sometimes called “bulk” temperature errors) and gradients are captured in the “thermal errors” term. The third term above SXT Mirror, “launch shifts”, captures errors associated with the launch. These errors are typically non-elastic effects brought on by launch loads. An allocation of 2 arc-seconds, HPD, has been made for these errors.

The roll-up term “SXT FMA, on-orbit performance”, is the RSS of the four terms immediately below it; SXT FMA, as built, material stability effects, thermal errors and SXT FMA launch shifts. It is 12.48 arc-seconds, HPD, and represents the on-orbit imaging performance of the SXT at end-of-life.

The next five terms up from “SXT FMA, on-orbit performance”, are “Telescope Level” errors. These are errors associated with operation of the SXT as a telescope with a detector at one end of an optical bench and the SXT at the other end. The “SXT/SI Focus Error” term, 0.2 arc-seconds HPD, is small since we have assumed the use of a focus mechanism to adjust the axial position of each science instrument (SI). The residual error term reflects the extent of our ability to compute the best focus position. Next we have an “SXT/SI misalignment” error term. This term is due to misalignment between the SXT optical axis and the telescope axis (line between the SXT node and detector mechanical center). It is a grouping of two error contributors; 1) tolerances in the alignment SXT/SI process and 2) imprecision in the knowledge of the SXT optical axis. These errors force us to use the SXT slightly off-axis, with resulting image resolution error, but with the x-ray image on the detector center. A small field-dependent defocus error is also introduced. The next telescope error term, “SXT/SI vibration effects”, captures the smearing of the image due to high frequency SI to SXT vibration, typically driven by reaction wheel imbalance. An allocation of 2 arc-seconds (HPD) is made for this error. The term “SXT/Telescope mounting strain” term, with a 2 arc-second (HPD) allocation captures the distortion errors generated when the SXT is attached to the optical bench. The next telescope level error term is for “Image reconstruction errors”. There are two separate error terms (not shown explicitly in the table) which RSS to the 4.24 arc-second (HPD) “Image Reconstruction” error term. Constellation-X science instruments are photon-counting detectors which record the position of each photon received on their respective focal planes. Attitude motion of the observatory during an observation will cause photons from the same source to land at different positions on the detector focal plane. This is corrected for, on a photon-by-photon basis, by using the star camera derived aspect solution. An “attitude knowledge drift” term represents the error in this correction process. A second image reconstruction error term is “SI/SXT focal plane drift”. Over the course of an observation the detector can move laterally with respect to the SXT node. This motion is primarily thermally driven optical bench “hot-dogging”, and occurs mainly when the sun-pitch attitude is changed. It generally stabilizes over time with a time constant of about 6-12 hours. Together, the two image reconstruction error terms RSS to 4.24 arc-seconds (HPD). Note: On Chandra the SI/SXT focal plane drift is measured with a Fiducial Light (FID) system and is largely corrected for. Constellation-X has less stringent angular resolution requirements and a more limited range of sun-pitch angles (compared to Chandra). A sub-allocation of 3 arc-seconds (HPD) was made for this error, which allows us to operate Constellation-X without a FID light system. The sub-allocation for attitude knowledge drift is also 3 arc-seconds (HPD). This error term could be reduced by a substantial amount by using a more accurate star camera; however we have assumed a lower cost star camera which is still consistent with Constellation-X requirements.

The “Telescope Level effects” terms RSS to 5.2 arc-seconds (HPD).

The angular resolution error budget now is split off into two separate budgets, one for the X-ray Micro-calorimeter System (XMS) or micro-calorimeter detector and another for the Reflection Grating Spectrometer (RG) 0th order image. The next error term (upwards) for the XMS is pixelization error, due to XMS detector pixel size of 5 arc-seconds. The “On-orbit Telescope (single satellite)” term is the RSS of pixelization error, telescope level effects and SXT FMA on-orbit performance. The final error term, “co-add 4 satellites”, captures the errors associated with adding the images from 4 satellites to create a single image. At the top level we see the XMS image resolution allocation of 14.16 arc-seconds (HPD), the requirement, 15 arc-seconds (HPD) and the margin vs. the requirement (in quadrature).

The RGS 0th order image resolution allocation is obtained as the RSS of four terms; “On-orbit telescope (from below), “grating resolution error”, “CCD detector pixelization error” and “Co-add error”. Grating resolution errors are due to the fact that each photon in the 0th order RGS image has been reflected off a grating element and is subject to errors in the grating. An allocation of 3 arc-seconds (HPD) is made for this term. CCD pixels which are used to readout the RGS 0th order image are smaller than micro-calorimeter pixels (0.5 arc-second) and the pixelization error term is smaller, at 0.41 arc-seconds (HPD). The RGS 0th order image resolution allocation is 14.48 arc-seconds (HPD) with a margin (in quadrature) of 3.92 arc-seconds (HPD) vs. the 15 arc-second requirement.

2.2 Optical Segment Error Allocations

The optical elements are the largest terms in the budget, with an allocation of 9.9 arc-seconds (HPD). Error allocations for the following individual optics error terms are shown in Table 1.

1. Sag
2. Axial Figure
3. Roundness & Delta-Delta-R
4. Circularity
5. Average Radius & Cone Angle

2.2.1 Sag

The sensitivity to sag errors is large. If the sag errors on the P and H are of the same sign, the HPD is about 25 arc-sec for a 1.5 μm sag error (P-V) on each optic. If, however, the sag errors are of the opposite sign, they cancel and the sensitivity is almost zero. We believe that the sag terms will most likely be highly correlated (the worst case) and have based the error allocation on this assumption. The resulting error allocation is 0.12 μm Legendre coefficient error, or 0.18 μm P-V sag error on either the P or H.

2.2.2 Axial Figure Errors

Axial figure errors are the largest contributor to the error budget at approximately 9 arc-seconds, HPD. In the interest of understanding error budget requirements we artificially separate axial figure error in low and mid spatial error frequencies. Low spatial frequency errors geometrically deviate the incident x-rays, producing a blur circle whose diameter is proportional to the root mean square (rms) slope of the errors. Assuming a Gaussian distribution of slope error, the resulting HPD from two uncorrelated reflectors is a factor of 3.84 ($= 2 \times 2 \times \sqrt{2} \times 0.68$) times the rms slope error. (One factor of 2 accounts for reflection, the second factor of two converts from radius to diameter, the factor of $\sqrt{2}$ accounts for two uncorrelated sets of optic errors, and the factor of 0.68 converts from an rms diameter to a half power diameter).

Mid spatial frequency errors scatter the incident x-rays. The scattered fraction the Strehl factor S , is a function of the rms amplitude of the error,

$$S = \exp(-(2k\sigma\sin\alpha)^2)$$

where $k = \text{wavenumber} = 2\pi/\lambda$, λ is the wavelength of the incident light, σ is the (two surface) rms amplitude, and α is the grazing angle. The fraction of light that is not scattered by mid frequencies is $1-S$. The angular deviation of the scattered light is given by the grating equation, whose grazing angle, small angle approximation is:

$$\lambda = d\theta \cdot \sin\alpha$$

where d is the error spatial period and θ is the ray deviation due to scatter. The scattered light distribution resulting from the mid-spatial frequency errors is convolved with the specular core from the low spatial frequency errors, and added to the specular core from light which does not scatter. For the simple 1 dimensional case we express this as:

$$\frac{dI}{d\theta}_{total} \approx (1-S) \cdot \frac{dI}{d\theta}_{specular} + S \cdot \frac{dI}{d\theta}_{specular} \otimes \frac{dI}{d\theta}_{scatter}$$

We have begun the process of flowing down the axial figure requirement to low, mid, and high frequency (roughness) bandwidths. In general, the rms slopes and amplitudes over these bandwidths will be dependent upon the shape of the error power spectrum density (PSD). Preliminary flowdown using some "strawman" PSDs yields an rms slope error requirement of ~ 1 arc second for error frequencies less than 0.02 mm^{-1} , and a bandwidth limited rms amplitude requirement of ~ 80 Angstroms for frequencies between 0.02 and 1 mm^{-1} .

Planned axial figure error flowdown will focus on (a) refining the surface error PSDs and (b) flowing down that requirement to various optic manufacturing processes. The latter step is necessary as a guide to successfully fabricating the optics. For example, the currently envisioned two-step fabrication process of slumping a glass substrate followed by epoxy replication² will necessitate different PSD requirements for the slumping and replication mandrels. In addition, those mandrel requirements will also be a function of the process – replication "smoothes" higher spatial frequency errors residual from slumping so the slumping mandrel can be coarser at higher frequencies than the final optic figure.

2.2.3 Roundness and Delta-Delta-R Errors

We expect that the as-manufactured optics will have roundness and $\Delta\Delta R$ errors, and have assumed roundness and delta-delta-R errors at frequencies which are 3, 6, 12 and 240 (where θ is the optic azimuth which runs from ~ 5 degrees to ~ 55 degrees for the current OAP). The effects these errors on HPD have been analyzed. The following random terms were assumed:

- 3 theta roundness (μm)
- 3 theta delta-delta-R (arc-seconds)
- 6 theta roundness (μm)
- 6 theta delta-delta-R (arc-seconds)
- 12 theta roundness (μm)
- 12 theta delta-delta-R (arc-seconds)
- 24 theta roundness (μm)
- 24 theta delta-delta-R (arc-seconds)

The sensitivities to these terms are given in Table 1 as 0.15 arc-seconds (HPD) per $1 \mu\text{m}$ (P-V) roundness error, and 3.5 arc-seconds (HPD) per arc-second (P-V) $\Delta\Delta R$ error. Allocations for roundness of $5 \mu\text{m}$ and for $\Delta\Delta R$ of 0.71 arc-seconds were made, with HPD contributions of 0.75 and 2.47 arc-seconds, respectively.

2.2.4 Replicated Optics Circularity Errors

The replicated optical elements have a roundness error which is near zero at the center azimuth and grows monotonically (of either sign) towards the edges. This error has been modeled as:

$$\text{Error} = \text{circ1} * (1.0 - \sin(3\theta)) \quad 0 < \theta \leq 30$$

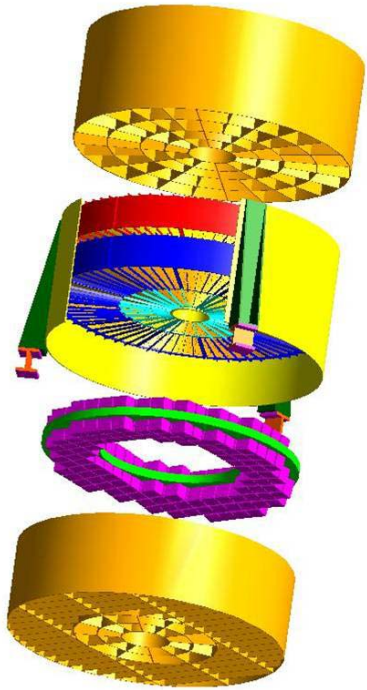
$$\text{Error} = \text{circ2} * (1.0 - \sin(30)) \quad 30 < \theta \leq 60$$

circ1 and circ2 are each independently chosen random numbers with a sigma of 7 μm , resulting in an RSS sum of 9.9 μm . The HPD which resulting from these errors has a 1σ of 0.28 arc-seconds.

2.2.5 Average radius and cone angle errors

The average radius and average cone angle of the formed optical segments are typically not equal to the design values. Our assembly and alignment procedure, however, corrects for these errors. The optical segments are placed into the housing and adjusted to the correct radii, top and bottom. These adjustments correct the radius and cone angle, but also introduce some distortion in the optical figure. An allocation of 5 arc-sec (HPD) is made in the budget for these effects, captured in the term “installation in housing”. To meet this allocation, we must control the as-manufactured radius and cone angle to within the tolerances shown in Table 1.

2.3 Flight Mirror Assembly and Alignment Allocations



After fabrication, the optical elements are assembled into the Flight Mirror Assembly (FMA). A conceptual drawing of the FMA is shown in Figure 2. As described in Reference 1, the FMA contains 36 wedge shaped modules; 18 primary modules and 18 secondary modules. The 18 primary modules include six 60 degree inner modules and 12 30 degree outer modules. The 18 secondary modules also include six 60 degree inner modules and 12 30 degree outer modules. Each individual module contains many optical segments. Outer modules have approximately 90 25 degree optical segments. Inner modules contain approximately 130 55 degree optical segments. The segments within each module must be aligned to each other, and corresponding primary and secondary modules must be aligned to each other so as to form an x-ray image at the telescope focus. The FMA may be thought of as being composed of 18 wedge-shaped module pairs, with the primary and secondary modules in a pair aligned to each other and the 18 wedge pairs aligned to each other to form a complete FMA.

Figure 2 – Constellation-X Flight Mirror Assembly (FMA)

2.3.1 Assembly and Alignment Overview

Although many of the assembly and alignment details are not yet final, an outline of this process has been constructed for error budgeting purposes. A strawman assembly and alignment process would follow the following steps:

1. Install the primary optical segments in each of the modules, time sequenced as needed to support FMA assembly.
2. Align segments within each primary module to each other and fix in place with epoxy bonds.

3. Install the secondary optical segments in each of the modules, time sequenced as needed to support FMA assembly.
4. Setup the primary and secondary modules together in the alignment tower.
5. Align each secondary optical segment to its corresponding primary segment and fix in place by epoxy bonds.
6. Repeat this process for all primary-secondary pairs.
7. Setup the FMA flight housing in the alignment tower.
8. Install and align each of the primary and secondary module pairs into the housing, aligning each secondary module to its corresponding primary and to an alignment reference mirror plus the ensemble of previously installed module pairs.
9. Fix each module into the FMA housing by epoxy bonding.
10. Install the thermal pre-collimator.
11. Install the Reflection Grating Assembly (RGA) grating modules.
12. Install the thermal post-collimator.
13. Finish FMA assembly by installing thermal control components, and interface mounting hardware.

Given this strawman assembly sequence, we have made allocations (see Figure 1) for assembly and alignment errors in four major categories:

1. Errors due to installation of optical segments into the module housings.
2. Alignment errors
3. Errors due to bonding strain
4. Errors due to gravity release (assemble and align in a 1G field and operation at 0 G).

Optical Elements - Budget Allocations					
Error Term	Allocation	Sensitivity	Allocation	Units	Definition
	HPD	HPD/Unit	Unit		
Optical Elements-Total	9.90				
Sag	3.00	25.00	0.12	μm	Peak-Valley
Axial Figure	9.07	3.84	2.36	arc-sec	RMS Slope errors
Roundness	0.75	0.15	5.00	μm	Peak-Valley
ΔΔR	2.47	3.50	0.71	arc-sec	Peak-Valley
Circularity	0.28	0.03	9.90	μm	See 2.2.4
Average Radius	0.00	0.00	±33.00	μm	See 2.2.5
Cone Angle	0.00	0.00	±10.00	arc-sec	See 2.2.5

Table 1 – Optics Error Allocations

3. OPTICAL ASSEMBLY PATHFINDER II - OVERVIEW

The Constellation-X project is actively pursuing technology development in many technical areas. One of the most important is the development of the Spectroscopy X-Ray Telescope. A technology development program is being pursued with the intent of demonstrating technical readiness prior to the program new start. Key elements of the program include the replication of the optical elements, assembly and alignment of the optics into a complete mirror assembly and

demonstration of production techniques needed for fabrication of multiple units. These elements will be demonstrated in a series of engineering development and prototype optical assemblies which are increasingly flight-like.

During the past year we have developed two Optical Assembly Pathfinder (OAP) Units, OAP1 and OAP2. OAP1, as described in Reference 11, was developed as a mechanical pathfinder to explore assembly and alignment techniques. OAP2, as described in Reference 10, is being developed to demonstrate end-to-end performance by X-ray testing¹².

In the past year, the OAP1 has been used at GSFC to develop and demonstrate assembly and alignment techniques. The OAP1 effort includes two wedge-shaped modules, each with 10 precision radial adjusters (five on each end of the 200mm long optical segment). The OAP2 has been developed to make use of the alignment capabilities of OAP1 but in

an assembly which will undergo x-ray testing. The OAP2 is shown in Figure 3. It consists of two titanium housings, each containing a single optical segment (primary or secondary). As described in [10], each of the housings fits within the larger OAP1 housing and the OAP1 optic adjusters are used to align optics within the OAP2. After alignment is achieved, the optical segments are bonded to the 10 radial struts (five on either end of each segment) which are part of OAP2. After optic installation, the two OAP2 housings are bonded together using the “T” shaped beams as shown in Figure 3. Figure 3 shows the complete OAP2 in its X-ray test orientation, optical axis horizontal and optics orientation as shown.

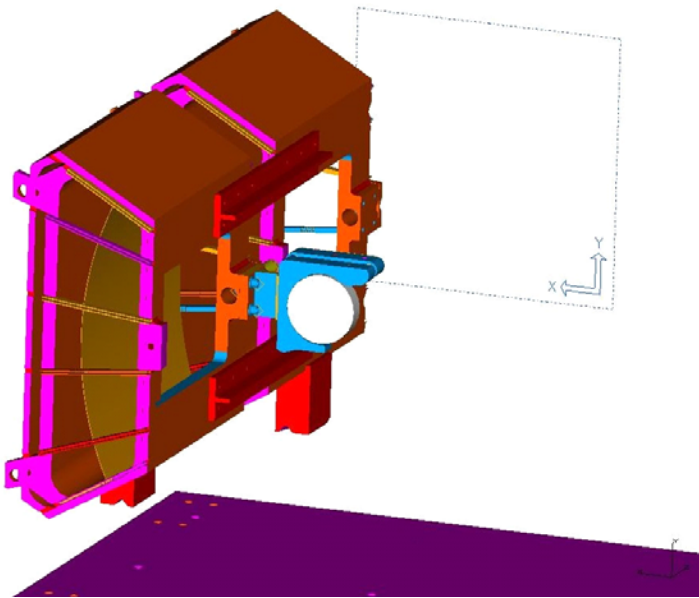


Figure 3 – OAP2 With Kinematic Mount

4. OPTICAL ASSEMBLY PATHFINDER II – EXPECTED PERFORMANCE

4.1 OAP2 Performance Prediction

The OAP2 X-ray test performance prediction is shown in Figure 4. This prediction has elements in common with the SXT FMA, but also has elements unique to the OAP2 and its x-ray test configuration. The “OAP2 as-built” configuration has the same elements and estimated performance as the “SXT FMA, as built” error budget allocation, 12.07 arc-seconds (HPD). This includes the optical elements, housing installation, alignment errors, bonding strain and gravity release. The main reason for this is that analysis and test activity in support of the OAP2 effort has been carried over into the SXT FMA error budget process. Another reason is that we have made it a goal that the OAP2 optical segments have flight-level performance.

Continuing upwards in the prediction, the material stability effects estimate is the same as the SXF FMA allocation (1 arc-second HPD). At this level the OAP2 prediction departs from the SXF FMA error budget. In place of SXF FMA Telescope level effects, detector effects and the effect of adding together four images from separate satellites, we have OAP2 specific thermally driven errors and X-ray test errors. The thermally driven errors include the effects of an average temperature offset on the OAP2 unit and also on the epoxy replicated optical segments, and also the effects of thermal gradients on three axes. The X-ray test errors include gravity distortion, test equipment error, finite source error

and x-ray source spot size error. The top level prediction for the x-ray test is a half power diameter of 14.34 arc-seconds. The OAP2 unique errors will be described in more detail in Section 5.

5. OAP2 THERMALY INDUCED ERRORS

5.1 OAP2 Thermally Driven Errors

The OAP2 will have performance degradations due to operation at off-nominal average temperatures (“thermal soak”) and the presence of thermal gradients. Analyses of these effects have been made over the past year. A combination of finite element modeling (see Figure 5) plus optical raytracing has provided sensitivities to temperature differences and gradients. Five thermally driven errors are included as error terms in the OAP2 performance prediction:

- 1) Thermal soak – Effect of OAP2 operation at an overall average temperature different from the average OAP2 assembly temperature. Distortions caused primarily by mis-match in CTE between glass and housing.
- 2) Epoxy bi-layer effects - Effect of OAP2 operation at an overall average temperature different from the optic fabrication temperature. Distortions caused by mis-match of epoxy and glass CTE. Due to the use of a glass-epoxy bi-layer optic.
- 3) Axial Temperature Gradient – Effects of a temperature variation along the OAP2 optical axis (Z axis in Figure 5). Analysis assumes a linear gradient over entire OAP2, front end of primary housing to back end of secondary housing.
- 4) Transverse Temperature Gradient – Effects of a temperature variation normal to the OAP2 optical axis and in the X-ray test horizontal plane (Y axis in Figure 5). Analysis assumes a linear gradient from the inner to outer OAP2 housing walls.
- 5) Vertical Temperature Gradient – Effects of a temperature variation normal to the OAP2 optical axis and in the X-ray test vertical plane (X axis in Figure 5). Analysis assumes a linear gradient over OAP2 housings, top to bottom.

The HPD sensitivities, temperature tolerances and contributions to the OAP2 error budget are shown in Table 2. The RSS of all five thermal terms is 1.48 arc-seconds. The tightest thermal control tolerance is the transverse gradient tolerance of 0.1 degrees C. Given these thermal control requirements, an OAP2 thermal control system has been fabricated, as discussed in Reference 12.

Error Term	HPD Sensitivity	Tolerance	Contribution	Comment
	arc-sec per deg C	(deg C)	(arc-sec)	
Thermal soak, per C	0.3	1.0	0.3	
Epoxy Bi-layer effects, per C	1.0	1.0	1.0	20μm EP301/400μm glass
Axial Gradient (Z in Figure 5)	0.2	0.5	0.1	
Transverse Gradient (Y in Figure 5) (Ti bars join P & H Hsgs)	7.3	0.1	0.73	
Vertical Gradient (X in Figure 5)	1.5	0.5	0.75	
RSS			1.48	

Table 2 – Thermal Results Summary

Contributors (HPD - arcsec)	Estimate/Prediction				Rationale/Comments
Image Resolution – OAP2 X-Ray Test	14.34				RSS
X-Ray Test Errors		7.42			RSS
Gravity Distortion			7.00		
Test Equipment errors			1.00		
Finite Source Distance			1.00		
X-ray Source spot size			2.00		1 mm spot
OAP2 Thermally Driven Errors		1.48			RSS
Average Temperature Offset			0.30		1 Degree C Temperature offset
Epoxy/glass bi-layer effects			1.00		20µm EP301/400µm glass, 1 Degree C Offset
Axial Gradient			0.10		0.5 degree end-to-end gradient
Transverse Gradient			0.73		0.1 degree inner wall to outer wall gradient
Vertical Gradient			0.75		0.5 degree top to bottom gradient
Material Stability effects		1.00			Estimate
OAP2 As Built		12.07			Analysis
Gravity release			1.50		FEA analysis using vertical assy
Bonding strain			3.00		Eng. estimate, analysis in process
Alignment errors (using CDA)			3.38		RSS
CDA Dynamic Accuracy				0.76	
CDA Static Accuracy				1.68	
Thermal Drift				2.00	
Adjustment Accuracy				2.00	
Installation in housing			5.00		Est. based on OAP1 testing
Optical elements			9.90		Est. based on tech dev program

Figure 4 – OAP2 X-ray Test Performance Prediction

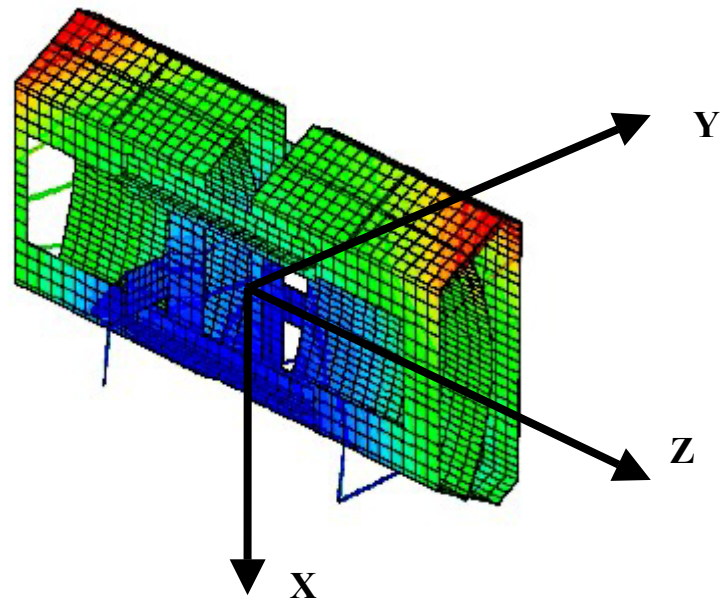


Figure 5 – OAP2 Finite Element Model

6. OPTICAL ASSEMBLY PATHFINDER II GRAVITY ERRORS

6.1 OAP2 Gravity Errors - Overview

The effects of gravity on OAP2 assembly and alignment and on x-ray test results were analyzed during the design the OAP2. Finite element modeling of the OAP2 was used in conjunction with optical raytracing to predict the effects of gravity on assembly and to select the optimal x-ray test orientation. A summary of these results is given in Table 3. We predict that assembly in the vertical orientation will add 1.5 arc-seconds (HPD) in quadrature to the overall HPD of the OAP2. Two x-ray test configurations were analyzed; 1) “flat” and 2) “on-edge” (see Figure 8). The “on-edge” configuration was selected since it had less gravity induced error in the x-ray test.

Load Case	HPD(50 Deg Aperture)
1G Vertical, baseline support	1.5
1G On edge (baseline)	7.0
1G flat	17.6

Table 3 – OAP2 Gravity Results

6.2 Assembly Support Condition

The FEA model of the assembly configuration is shown in Figure 6 and a view of the alignment and assembly configuration and GSE is shown in Figure 7. The OAP2 assembly plan is as follows:

1. Install P and H housings with optics on two sets of three point supports.
2. Rough-align optics in P and H housings using OAP1 housing and adjusters.
3. Install “T” beams between P and H housings using assembly GSE.
4. Perform final alignment of optics using OAP2 adjusters and bond to P and H housings.

Given this assembly sequence, the strain which is present during final optic bonding will be locked into the optics and represents the “assembly strain” portion of the error budget (3 arc-second allocation). FEA results indicate a 1.5 arc-second HPD contribution from assembly in this configuration.

6.3 X-Ray Test Support Condition

Two configurations for the x-ray test have been considered, the “edge” and the “flat” configurations, as shown in Figure 8. Our analyses have led to the choice of the “edge” x-ray test configuration, since its performance is better than the “flat”. During x-ray testing the OAP2 will be supported on a 3 point kinematic mount as shown in Figure 3. The 1G structural distortion contribution to HPD in the on-edge x-ray test is 7.1 arc-seconds at the nominal 50 degree aperture. This may be reduced to under 4 arc-seconds by use of a 30 degree aperture.

The optic slope distortions are shown in Figure 9. Since they are highly localized we can verify our performance modeling in the x-ray test by sampling apertures of various widths and azimuthal locations. Raytrace predictions of the 1G performance effects for various apertures are listed in Table 1. The overall HPD due to the 1G effect over a full 50 degree aperture is 7.1 arc-seconds.

Aperture	HPD(arc-sec)
50 Degrees (65-115)	7.1
2 Degrees (65-67)	76.6
2 Degrees (69-71)	36.4
2 Degrees (79-81)	11.1
2 Degrees (89-91)	0.3

Table 4 – HPD Variation with Aperture

However, if we limit the aperture azimuthal width to only 2 degrees, the HPD values will vary by large amounts as we move the 2 degree aperture to various positions within the full aperture. At the edge of the optic we get 76 arc-seconds HPD while we get 0.3 arc-seconds in the center. In the x-ray test we will scan the azimuthal extent of the aperture using our motorized aperture wheel and 2 degree aperture. The effects of 1G should be evident even in the presence of other large errors. Figure 9 shows raytrace spot diagrams for four of the cases listed in Table 4. The long radial form of the “2 degree aperture at the edge” image is a result of the errors in axial slope sampled over a narrow aperture. Image resolution improves as the 2 degree aperture is moved towards the center of the full aperture, also shown in Figure 9. Results for the full 50 degree aperture are also shown. The most prominent features are the large spokes generated by edge effects; however the bulk of the power is contained in a much smaller region near focus.

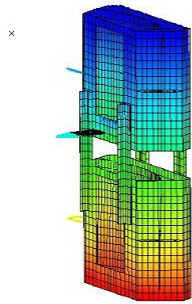


**Figure 6 – FEA Model of OAP2
Assembly Configuration**

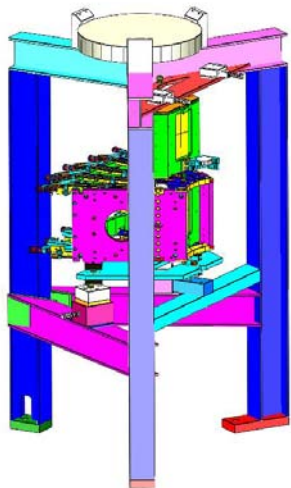
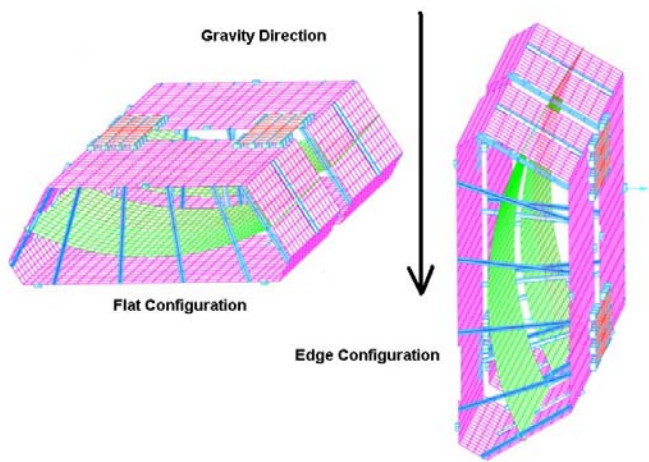
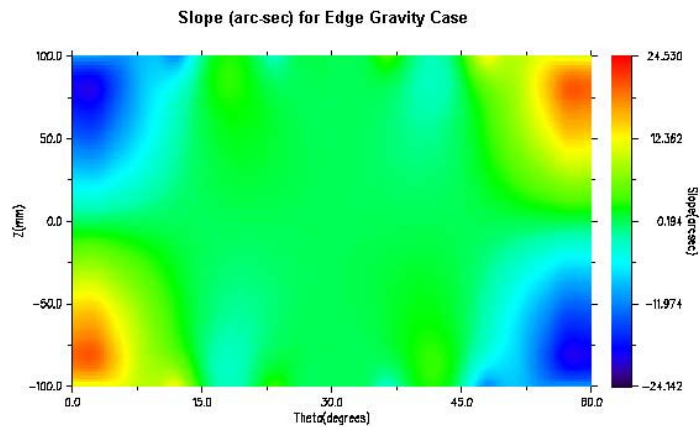


Figure 7 – Assembly Configuration and Tower GSE



**Figure 8 – Two Candidate X-Ray Test Mounting
Configurations**



**Figure 9 – Slope Distortions for Primary
Optic in Edge Mount**

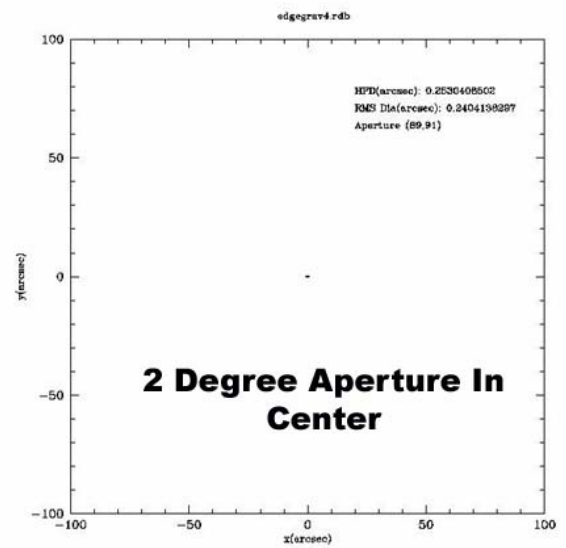
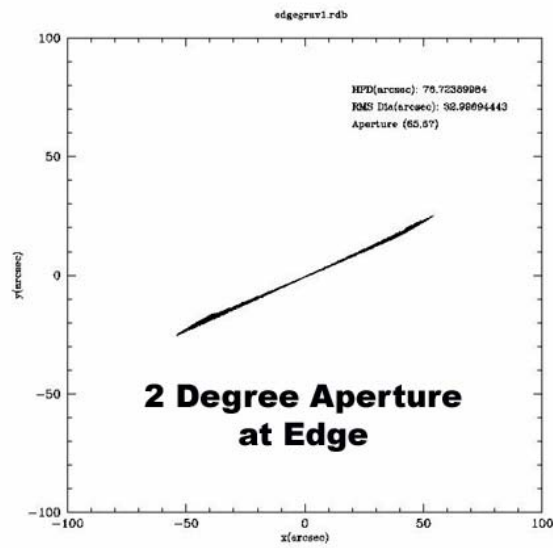
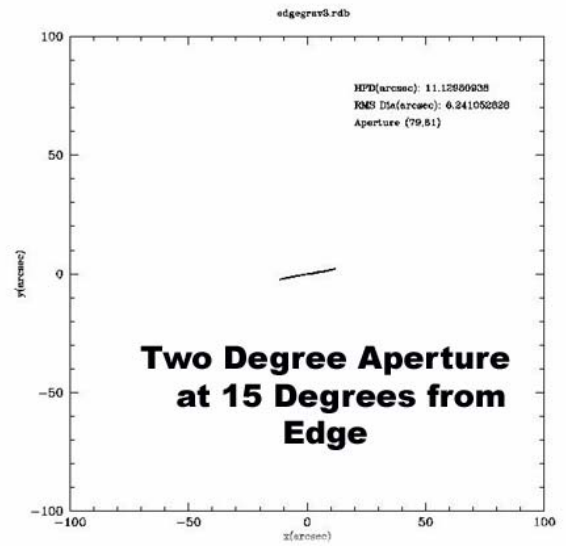
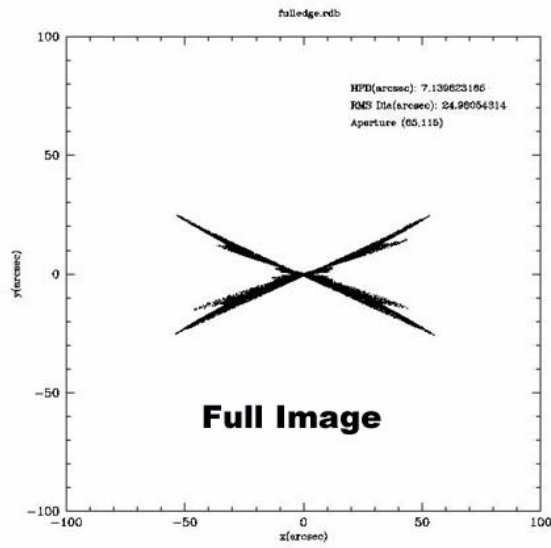


Figure 9 – OAP2 Raytrace Results for Variable Aperture Positions

7. REFERENCES

1. R. Petre, W. W. Zhang, D. A. Content, T. T. Saha, J. Stewart, J. H. Hair, D. Nguyen, W. A. Podgorski, W. R. Davis, Jr., M. D. Freeman, L. M. Cohen, M. L. Schattenburg, R. K. Heilmann, Y. Sun, C. Forest, "Constellation-X spectroscopy x-ray telescope (SXT)", SPIE 4851-50
 2. W. W. Zhang, K. Chan, D. A. Content, R. Petre, P. J. Serlemitsos, T. T. Saha, Y. Soong, "Development of mirror segments for the Constellation-X observatory", SPIE 4851-58
 3. G. P. Monnelly, D. Breslau, N. Butler, C. G. Chen, L. M. Cohen, W. Gu, R. K. Heilmann, P. T. Konkola, O. Mongrard, G. R. Ricker Jr., and M. L. Schattenburg, "High-Accuracy X-Ray Foil Optic Assembly", Proc. SPIE 4138, 164 (2000).
 4. C. G. Chen, L. M. Cohen, R. K. Heilmann, P. T. Konkola, O. Mongrard, G. P. Monnelly, and M. L. Schattenburg, "Micro-Comb Design and Fabrication for High-Accuracy Optical Assembly", J. Vac. Sci. Technol. B 18, 3272 (2000).
 5. P. E. Glenn, "Centroid detector assembly for the AXAF-I alignment test system", SPIE 2515, pp352-360 (1995)
 6. Hair, J. Stewart, R. Petre, W. W. Zhang, D. A. Content, T. T. Saha, W. A. Podgorski, P. E. Glenn, M. L. Schattenburg, R. K. Heilmann, Y. Sun, G. Nanan, "Constellation-X soft x-ray telescope segmented optic assembly and alignment implementation", SPIE 4851-76
 6. Recent progress on the Constellation-X spectroscopy x-ray telescope (SXT) (Invited Paper), R. Petre, NASA Goddard Space Flight Ctr. [5168-21]
 7. Fabrication of segmented Wolter type-1 mandrels for the Constellation-X mirror development program, W. J. Egle, W. Hafner, A. Matthes, G. Willma, A. Ilg, H. Schiehle, Carl Zeiss Laser Optics GmbH (Germany) [5168-18]
Development of mirror segments for the Constellation-X mission, W. W. Zhang, NASA Goddard Space Flight Ctr. [5168-19]
 8. Optical metrology for the segmented optics on the Constellation-X soft x-ray telescope, D. A. Content, D. Colella, C. Fleetwood, T. Hadjimichael, T. Saha, G. Wright, W. Zhang, NASA Goddard Space Flight Ctr. [5168-23]
 9. Noncontact metrology on segmented x-ray optics for the Constellation-X SXT, T. Hadjimichael, Swales Aerospace; D. Content, G. Wright, NASA Goddard Space Flight Ctr.; C. Fleetwood, Swales Aerospace; D. Colella, ManTech International; T. Saha, W. Zhang, NASA Goddard Space Flight Ctr. [5168-24]
 10. Constellation-X SXT optical alignment Pathfinder 2: design, implementation, and alignment, S. M. Owens, J. J. Hair, NASA Goddard Space Flight Ctr.; W. A. Podgorski, Harvard-Smithsonian Ctr. for Astrophysics; P. Glenn, Bauer Associates, Inc.; J. Stewart, G. Nanan, T. T. Saha, R. Petre, W. W. Zhang, D. A. Content, NASA Goddard Space Flight Ctr. [5168-27]
 11. Constellation-X Spectroscopy X-ray Telescope Assembly and Alignment, W. A. Podgorski, D. Content, P. Glenn, J. Hair, R. Petre, T. Saha, M. Schattenburg, J. Stewart, W. Zhang, [4851-57]
 12. X-ray testing Constellation-X optics at MSFC's 100-m facility, S. L. O'Dell, M. A. Baker, NASA Marshall Space Flight Ctr.; D. A. Content, NASA Goddard Space Flight Ctr.; M. D. Freeman, Harvard-Smithsonian Ctr. for Astrophysics; P. Glenn, Bauer Associates; M. V. Gubarev, Univ. Space Research Association; J. H. Hair, NASA Goddard Space Flight Ctr.; W. D. Jones, M. K. Joy, J. E. McCracken, NASA Marshall Space Flight Ctr.; G. Nanan, Swales Aerospace; S. M. Owens, R. Petre, NASA Goddard Space Flight Ctr.; W. A. Podgorski, Harvard-Smithsonian Ctr. for Astrophysics; B. D. Ramsey, NASA Marshall Space Flight Ctr.; T. T. Saha, J. W. Stewart, NASA Goddard Space Flight Ctr.; D. A. Swartz, Univ. Space Research Association; W. W. Zhang, NASA Goddard Space Flight Ctr.; G. X. Zirnstein, Univ. Space Research Association [5168-34]
-